

# GCM SIMULATIONS OF NORTHERN SUMMER DUST STORMS OBSERVED BY THE PHOENIX LIDAR

**F. Daerden**, Belgian Institute for Space Aeronomy, Brussels, Belgium ([frank.daerden@aeronomie.be](mailto:frank.daerden@aeronomie.be)), **J. Whiteway**, Center for Research in Earth and Space Science, York University, Toronto, Canada , **L. Neary**, Belgian Institute for Space Aeronomy, Brussels, Belgium , **M. Lemmon**, Atmospheric Sciences Department Texas A&M University, College Station, Texas, USA , **B. Cantor**, Malin Space Science Systems, San Diego, California, USA , **M. Wolff**, Space Science Institute, Boulder, Colorado, USA , **E. Hébrard**, Laboratoire d'Astrophysique de Bordeaux, Floirac , France .

## Introduction:

The LIDAR instrument on the Phoenix Mars lander provided measurements of atmospheric dust profiles with unprecedented detail over a period stretching from late spring to late summer in the northern subpolar region on Mars (Whiteway et al. 2009). Around northern summer solstice enhanced dust loading was measured in the residual Planetary Boundary Layer (Komguem et al. 2013), with sometimes detached dust layers above the PBL. The enhanced dust activity around solstice is supported by measurements from the SSI instrument on the lander and by MARCI and CRISM from orbit (Cantor et al. 2010, Tamppari et al. 2010, Ellehoj et al. 2010).

A 3D GCM is applied to understand the origin of these high dust opacities. One component of the dust (the more uniform background loading) is found to come from local contributions by dust devils, which reach a maximal activity before and until solstice. The second component (the peaks) is found to come from dust lifted near the polar cap and transported into the Phoenix site. This second component is also found to be responsible for the detached layers sometimes observed by the LIDAR.

The GCM is able to simulate local dust storms around northern summer solstice near the edge of the polar cap, and these are confirmed by MARCI images. These dust storms are mainly the result of two factors: 1) when the seasonal CO<sub>2</sub> cap is shrinking to within the size of the permanent water cap, the thermal contrast between ice cap and surrounding soil is maximal, leading to strong near-surface friction velocities which can lift dust, and 2) the inclusion of a detailed roughness length map (Hébrard et al. 2012) in the GCM, along with a subgrid scale approach to handle the small scale roughness variability within the coarser GCM resolution.

The source of the dust around the permanent cap is likely related to sublimation lag becoming exposed after the evaporation of the cap and possibly also to the north polar dune fields.

## The GEM-Mars 3D GCM:

The Global Environmental Multiscale model for Mars (GEM-Mars) is a 3D gridpoint global circulation model (GCM) for Mars based on the terrestrial community model GEM, which is used for operational weather forecasting by the Meteorological Service of Canada (Coté et al. 1998). A first version of GEM adapted for Mars was the GM3 model of Moudden and McConnell (2005). New physics routines were added by Akingunola (PhD, 2008) and since 2009 at the Belgian Institute for Space Aeronomy. GEM-Mars is typically run on a 4°x4° uniform grid and has 102 hybrid levels ranging from the surface to ~150 km. GEM-Mars has an interactive 14 layer soil model including a subsurface ice table, a surface layer treatment following Monin-Obukov similarity theory, a parameterization for the convective boundary layer (Holtslag and Boville, 1993), active dust-, CO<sub>2</sub>-, pressure- and water cycles, a low level blocking scheme and gravity wave drag parameterization (Zadra et al. 2003), and online photochemistry (Garcia-Munoz et al. 2005, Neary et al., this workshop).

Routines for active dust lifting by saltation and dust devils were recently implemented in GEM-Mars (Daerden et al. 2013). These followed the approaches of Newman et al. (2002) and Kahre et al (2006). A difference with those approaches is that now a detailed map for aerodynamic roughness length (Hébrard et al. 2012) is implemented in GEM-Mars. In order to manage the high resolution geophysical fields (albedo, thermal inertia, roughness length) in the framework of the coarser GCM, subgrid scale treatments were developed based on a histogram method. To take into account sub-timescale variability, near-surface wind gustiness was implemented using a Weibull distribution.

The atmospheric dynamics simulated in GEM-Mars has been evaluated using measurements from the Viking Landers, MGS/TES, MOD/GRS, MRO/MCS, MRO/CRISM and Phoenix/MET. Figure 1 shows the near-surface temperature measured by the PHX/MET sensor at 2 m elevation and the

corresponding model result.

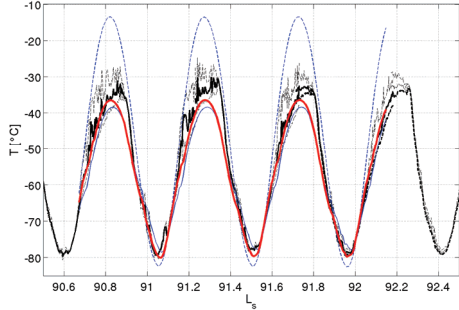


**Figure 1:** Temperature at 2 m above ground from the Phoenix MET sensor (black full, including daytime variability: black dashed) and as simulated by GEM-Mars (red: 2 m, blue dashed: surface, blue full: 30 m).

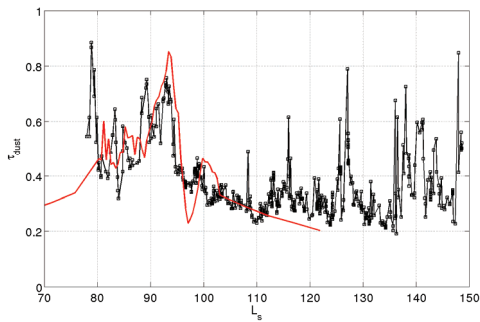


**Figure 2:** Opacity at 991 nm measured over Phoenix by SSI (black) and the GEM-Mars simulation (red). Time resolution for the plotted model result is 1 sol around solstice and 10 sols beyond.

#### Dust lifting simulations:

The GCM was run for several Mars years starting from initial conditions coming from previous model runs. Special attention was given to an accurate simulation of the springtime retreat of the northern seasonal cap. If the cap's evolution is not well simulated, the GCM will not (or not timely) produce sufficiently large thermal contrasts and related friction velocities for saltation. This optimization effort is presented in Daerden et al. (this workshop).

The dust devil activity is simulated in the GCM following the parameterization of Renno et al. (2008), which is threshold-independent, and the dust mass flux is proportional to the sensible heat flux and the depth of the boundary layer. The dust loading over the Phoenix site coming from this source is increasing throughout springtime, and reaches a maximum around  $L_s=50^\circ$ . From then on the opacity is very slowly decreasing until midsummer, where it reaches a peak again before the polar cap starts covering the region. This dust forms a background of total visible opacity of  $\sim 0.3$  over the Phoenix site throughout the full mission ( $L_s=76^\circ\text{--}150^\circ$ ).

On top of this background dust opacity, many peaks have been detected by SSI, some reaching up to opacities of 0.8 (Figure 2). These can be attributed to local dust events or to larger scale dust storms, usually coming down from the polar area (e.g. Ellehoj et al. 2010). The largest peak activity periods are around solstice and towards the end of the mission, the latter is mainly due to ice clouds. Here we focus on the dust activity around solstice.

The GCM simulates many local dust lifting events (which can be called local storms) near the permanent cap just before solstice. Due to the thermal contrast between the retreating seasonal north polar cap and the surrounding soil, enhanced friction velocities and surface wind stress values are simulated southwards of the cap throughout spring. From around the time when the seasonal cap reaches the size of the water cap ( $L_s \sim 80^\circ$ ) the surface wind stress considerably increases. This comes from a combination of the fact that the seasonal cap is covering the water cap ( $\text{CO}_2$  ice has a higher albedo than the  $\text{H}_2\text{O}$  ice) and that the newly exposed soil surrounding the cap, the north polar sand sea or erg, has a very low albedo. This then results in a large thermal contrast and in a "sea-breeze"-like effect.

The simulation of dust storms was also facilitated by the inclusion of the detailed roughness map and wind gustiness. Within the north polar sand sea there is considerable small scale variability in the roughness length map (Hébrard et al. 2012). At locations of increased roughness length the surface wind stress can more easily reach the saltation threshold. Because we use the fully resolved map (at  $1/8^\circ$  resolution) the small-scale variability is taken into account in the coarser scale GCM. Although there is some uncertainty in the retrieval process of the roughness length at these latitudes (Hébrard et al. 2012), we can assume that in reality such small-scale variability may indeed exist.

The GCM does produce dust storms in regions where dust storm activity has been identified in MARCI images (Figure 3). Dust lifted by these local storms is accumulated in the atmosphere and transported over the planet by the global circulation, including into the Phoenix location. Figure 4 shows the zonal mean dust opacity in the GCM in comparison to individual dust opacity retrievals from CRISM.

After solstice the peaks decrease rapidly, with some small oscillations in the opacity which can be explained by remnant dispersed dust clouds which have travelled around the planet in this timeframe.

Such oscillations are also visible in the SSI measurements (Figure 2).

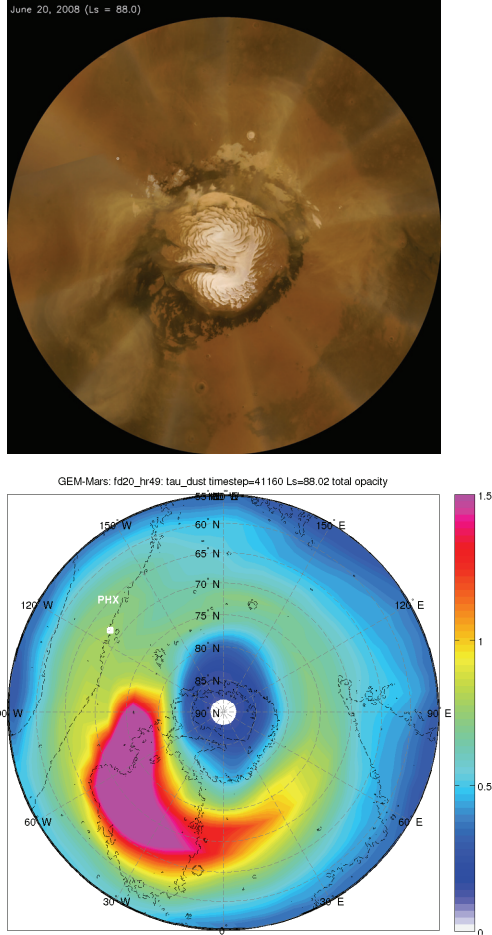


**Figure 3:** Top: MARCI mosaic image of June 20, 2008 ( $L_s=88^\circ$ ) showing a large dust cloud in the  $0^\circ$ - $90^\circ$ W quadrant. Bottom: GEM-Mars dust opacity map on the same day.

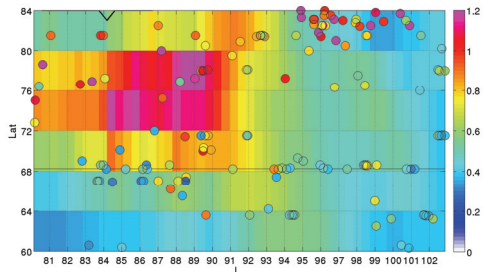


**Figure 4:** Zonal mean simulated dust opacity at 3hr resolution for the northern latitudes around solstice. Added (circles): individual (non-averaged) CRISM retrievals in the same time window in MY29.

#### LIDAR profiles:

Vertical profiles of dust optical extinction coefficient were derived from the Phoenix LIDAR measurements from a few hundred meters above ground to a maximum height of 15 km (Komguem et al. 2013). MCS dust extinction profiles (Kleinböhl et al. 2009, 2011) were selected on the same day as the LIDAR measurements and within 4 degrees in both latitude and longitude (this equals the GCM's resolution) from the Phoenix site. Due to opacity constraints in the lower part of the atmosphere, most of the MCS profiles are limited to about 10-15 km height. We scaled the MCS extinction profiles at 21  $\mu$ m by a factor of 7.3 to the LIDAR wavelength of 532 nm (Kleinböhl et al. 2011, Heavens et al. 2011).

The LIDAR and MCS dust extinction profiles match within measurement uncertainty around 15 km (Figure 5 and Figure 6). In addition GEM-Mars simulated dust extinction profiles were added. The overall consistency is very good. On one mission sol, sol 67, one co-located MCS profile penetrated into the PBL. The optical extinction matches well with the LIDAR profile there, as does the GCM result. Also the temperature profile of the GCM is consistent with the MCS temperature profile on that day (Figure 6).

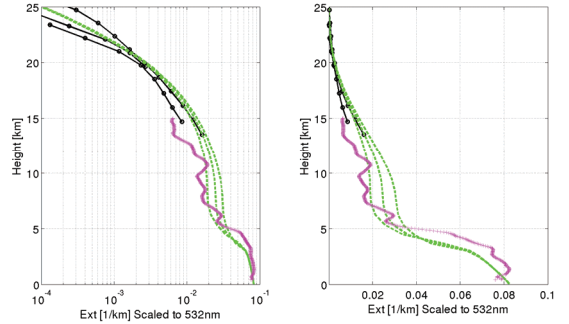


**Figure 5:** Comparison of the extinction profile on mission sol 32: LIDAR (pink), MCS (black) co-located within 4 degrees latitude and longitude, and some corresponding GEM-Mars profiles (green) interpolated to the MCS profiles. Left: log10 scale, right: linear scale (same data).

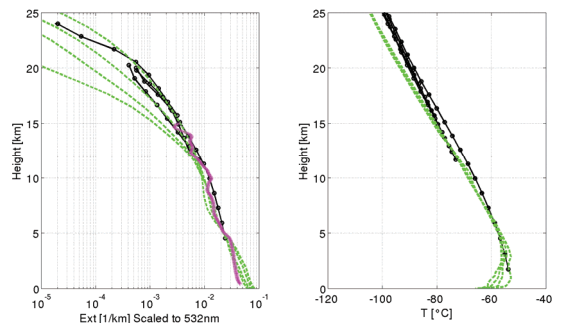


**Figure 6:** Left: Comparison of dust extinction

**profiles from: LIDAR (pink), MCS (black) and GEM-Mars (green) on mission sol 67 ( $L_s=107^\circ$ ). Right: comparison of temperature profiles from MCS (black) and GEM-Mars (green) for the same profiles.**

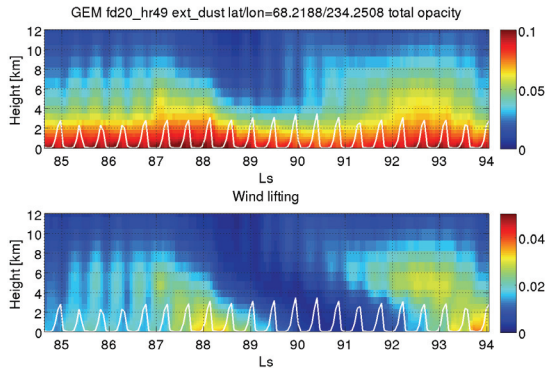


**Figure 7: Top: total simulated dust extinction over Phoenix around solstice. The PBL depth is also indicated (white). Bottom: only extinction of dust lifted by saltation.**

Around solstice the LIDAR also detected detached layers above the PBL. The GCM can explain these as layers of dust which are coming from the dust storms near the polar cap. In the northern latitudes where the dust is lifted, the PBL is very shallow and the dust enters the global circulation quite rapidly. It is advected at heights above the boundary layer over the planet and towards more southern latitudes, and while it sediments it slowly mixes into the boundary layer.

Figure 7 shows an example of this by separately showing the part of the dust over the Phoenix site which is attributed to saltation. Clearly layers of dust are entering into the Phoenix location above the PBL, and slowly sediment and mix with the dust in the local PBL in the course of a few sols.

### Conclusion:

By implementing parameterizations for dust lifting by dust devils and by saltation, in addition to a precise simulation of the northern seasonal cap retreat and by making use of a high-resolution aerodynamic roughness map, the GEM-Mars GCM simulates dust extinction profiles and opacities at the Phoenix location comparable to those measured by the Phoenix LIDAR and SSI instruments in the northern summer of MY29.

The dust variability can be explained by a combination of two sources: local dust devil activity and dust transported from local dust storms in the polar region. The simulated dust storms can be confirmed by MARCI images taken at the time of the mission.

### References:

- Akingunola, A. (2008), Martian Water Cycle Modeling with the Second Generation of the Global Mars Multiscale Model, PhD thesis, York University
- Cantor, B.A., et al (2010), MARCI and MOC observations of the atmosphere and surface cap in the north polar region of Mars, *Icarus* 208, 61–81
- Côté, J., et al (1998), The operational CMC-MRB Global Environmental Multiscale (GEM) model: Part I—Design considerations and formulation, *Mon. Weather Rev.*, 126, 1373–1395
- Daerden, F., et al. (2013), Dust lifting in GEM-Mars using a roughness length map, EPSC2013-206
- Ellehoj, M.D., et al. (2010), Convective vortices and dust devils at the Phoenix Mars mission landing site, *J. Geophys. Res.*, 115, E00E16
- García-Muñoz, A., et al. (2005), Airglow on Mars: Some model expectations for the OH Meinel bands and the O<sub>2</sub> IR atmospheric band, *Icarus* 176, 75–95
- Heavens, N. G., et al. (2011), The vertical distribution of dust in the Martian atmosphere during northern spring and summer: Observations by the Mars Climate Sounder and analysis of zonal average vertical dust profiles, *J. Geophys. Res.*, 116, E04003
- Hébrard, E., et al. (2012), An aerodynamic roughness length map derived from extended Martian rock abundance data, *J. Geophys. Res.*, 117, E04008
- Holtslag, A. A. M. and B. A. Boville (1993), Local versus non-local boundary-layer diffusion in a global climate model. *J. Climate*, 6, 1825–1842.
- Kahre, M. A., et al. (2006), Modeling the Martian dust cycle and surface dust reservoirs with the NASA Ames general circulation model, *J. Geophys. Res.*, 111, E06008.
- Kleinböhl, A., et al. (2009), Mars Climate Sounder limb profile retrieval of atmospheric temperature, pressure, dust, and water ice opacity, *J. Geophys. Res.*, 114, E10006.
- Kleinböhl, A., et al. (2011), A single-scattering approximation for infrared radiative transfer in limb geometry in the Martian atmosphere, *J. Quant. Spectrosc. Radiat. Transfer*, 112, 1568–1580
- Komguem, L., et al. (2013), Phoenix LIDAR measurements of Mars atmospheric dust, *Icarus* 223, 649–653
- Moudden, Y. and J.C. McConnell (2005), A new model for multiscale modeling of the Martian atmosphere, GM3, *J. Geophys. Res.* 110, E04001.
- Newman, C. E., et al. (2002), Modeling the Martian dust cycle, 1, Representations of dust transport processes, *J. Geophys. Res.*, 107(E12), 5123
- Tamppari, L. K., et al. (2010), Phoenix and MRO coordinated atmospheric measurements, *J. Geophys. Res.*, 115, E00E17.
- Whiteway, J.A., et al. (2009), Mars Water-Ice Clouds and Precipitation, *Science* 325, 68
- Zadra, A., et al. (2003): The subgrid-scale orographic blocking parametrization of the GEM Model, *Atmosphere-Ocean*, 41:2, 155-170.